Energy Conversion and Management 194 (2019) 94–111

Contents lists available at ScienceDirect

Energy Conversion and Management

journal homepage: www.elsevier.com/locate/enconman

Study on the combined operation of a hydro-thermal-wind hybrid power system based on hydro-wind power compensating principles

Yimin Wang, Mingzhe Zhao, Jianxia Chang*, Xuebin Wang, Yuyu Tian

State Key Laboratory of Eco-hydraulics in Northwest Arid Region of China (Xi'an University of Technology), 710048 Xi'an, China

ARTICLE INFO

Keywords:
Hydro-wind compensation
Combined optimal operation mode
Carbon dioxide emission
Power grid

ABSTRACT

The high randomness, intermittency and uncontrollability of wind power make large-scale wind power generation present large challenges for integration into a power grid. In this paper, the principles of hydro-wind compensating operation are explored, aiming at improving the power quality of wind power and promoting the integration of wind power into the power grid. Based on the principles of hydro-wind compensating operation, the calculation method of the hydropower compensation capacity for wind power is derived. Then, an optimizing operation model of a hydro-thermal-wind hybrid power system based on the hydro-wind power compensating principle is proposed to minimize the carbon dioxide emissions and obtain optimal operation scheduling of the hybrid power system by taking advantage of hydro-wind compensation and the peak regulation capacity of hydropower. In this model, the baseload and nonbaseload output emission rates are adopted to estimate the carbon dioxide emissions of different power output processes and the emission reduction benefits. Moreover, three scenarios of the operation mode are proposed to demonstrate the applicability of the hydro-wind power compensating principle in practice. The Northwest Power Grid in China is selected as a case study to verify the effectiveness of the proposed model compared to historical operating data. The results indicate that the hydro-wind power compensating principle plays a crucial role in hydro-thermal-wind combined optimal operation. Additionally, the proposed model can improve the wind power generation and reduce the carbon dioxide emissions of the power grid. In particular, the carbon dioxide emissions can be reduced by approximately $1696*10^4$ t each year in the Northwest Power Grid. This study provides an approach to schedule optimal operation plans for power grids with large-scale wind power and provides a valuable reference for the large-scale utilization of other kinds of renewable energy worldwide.

1. Introduction

Energy is the basic guarantee for economic and social development. With the gradual depletion of fossil energy and the increasing problem of climate change, resources and the environment are becoming increasingly important constraints on energy development. Meanwhile, it is urgent to improve the consumption of clean energy and reduce the proportion of coal and other fossil energy generation in the power grid. Therefore, interest in the use of renewable energy resources has been increasing. Wind and solar energy are considered major renewable resources. However, these new energy sources have the disadvantages of randomness, intermittency and uncontrollability. These disadvantages make large-scale wind power generation present large challenges for integration into the power grid [1]. Hydropower, by contrast, is advantageous in its rapid and adjustable response; the disadvantage of wind power can be made up by compensating operation of hydropower plants and wind power plants. Hence, cheap and clean hydropower compensates for uncertain wind power and reduces the dependence on thermal power, and this method is good for reducing emissions as well as costs [2]. Due to the amount of large-scale wind power integrated into the power grid, to consume the output and generation of wind power and ensure safe operation of the power grid, other power sources should regulate their output to compensate for wind power when the wind power output fluctuates. Therefore, it is important to develop a combined hydro-thermal-wind power generation system and strengthen research on the optimal scheduling of hydro-thermal-wind power systems. In this case, the study of a reasonably optimal scheduling of a hydro-thermal-wind power system is beneficial to realize the maximization of economic and safety benefits in the power grid.

As an important wind power and photovoltaic power generation base in China, the Northwest Power Grid has formed a situation of multipower sources combined operation. However, renewable energy

* Corresponding author.
E-mail address: chxiang@xaut.edu.cn (J. Chang).

https://doi.org/10.1016/j.enconman.2019.04.040
Received 24 December 2018; Received in revised form 9 April 2019; Accepted 11 April 2019

curtailment is becoming more frequent in the Northwest Power Grid, and the problems of wind power consumption and integration into the power grid are increasingly prominent. Hence, it is necessary to make full use of the peak load regulating capacity of hydropower plants for meeting the safe and stable operation of the power grid [3].

At present, multipower combined optimal scheduling is an active research field. The combined operation of multipower sources is considered an effective approach to solve the problem of wind power curtailment. Regarding the importance of supplying energy to regions that are far from the power grid, Amrollahi and Bathaee [4] analyzed and modeled a standalone power grid of hybrid photovoltaic/wind generation, Fang et al. [5] explored three major systems of smart microgrids (MGs) and smart protection systems and reviewed that MGs were capable of delivering power in more efficient ways by utilizing modern information technologies, and Hamdi Abdi et al. [6] reviewed and compared the objective functions, constraints, and methodologies of Optimal Power Flow applied to a hydro-thermal-wind hybrid power system of smart grids and micro-grids. However, these researchers aimed at multipower combined operation of smart micro-grids or a small regional power grid, which is unsuitable for multipower combined optimal scheduling for a large power grid.

Moreover, there are a very large number of applied studies on the optimized goals of operation scheduling of power systems and optimization techniques of multipower combined optimal problems. With increasing concern of environmental considerations, conventional pure economic scheduling no longer satisfies the requirements [7]. Society demand requires not only adequate and secure electricity at the cheapest possible price but also at a minimum level of emissions pollution. In [8], the economic emission, water transport delay and transmission loss of system load was considered to the daily hydrothermal scheduling. Zhang et al. [9] studied the cascade hydropower plants operation models considering comprehensive ecological water demands to quantitatively analyze the relationship between power generation and degree of ecological flow satisfaction. Chang et al. [10] developed the adaptive operation chart for the hydropower plant to mitigate climate change impacts, and to propose an optimal adaptive operation chart for cascade hydropower system to increase power generation under the climate change environment. Dubey et al. [11] developed the combined hydro-thermal-wind scheduling problem with five objectives consisting of cost, various emissions and power loss. In [12], the objective of the hydro-thermal-wind scheduling problem was to minimize the total system operational cost to meet the load demands during the intervals of the generation scheduling. Then, solving the power scheduling problem had been the theme of exhaustive exploration for years. The traditional mathematical methods include nonlinear programming, dynamic programming, and other modern heuristic stochastic search technique such as artificial neural network (ANN), evolutionary programming (EP), genetic algorithm (GA), differential evolution (DE), cultural algorithm (CA), particle swarm optimization (PSO). Nevertheless, the multipower combined optimal scheduling problem is difficult to solve. To address this problem, Meng et al. [13] proposed a new improved multi-objective cuckoo search (IMOCS) algorithm for solving the multi-objective hydropower station optimal operation (MOHSOO). Yuan et al. [14] integrated the chaotic sequence and genetic algorithm with a hybrid chaotic genetic algorithm to solve the short-term generation scheduling of a hydro system. For solution of short-term hydro thermal scheduling problems, Sinha et al. [15] developed the fast evolutionary programming (FEP) techniques. Yu et al. [16] compared different particle swarm optimization (PSO) techniques to solve the short-term hydro-thermal scheduling problem. In [17], an enhanced differential evolution algorithm was proposed to solve the daily optimal hydro generation scheduling problem. Guo and Peng [18] established the basic and characteristic equations for the hydropower system with surge tank, and investigated the safe and stable operation of hydropower system under step load disturbance. Yang et al. [19] proposed an algorithm for choosing gBest for each particle of the swarm from a Pareto-optimal solutions set. Then, various novel optimization techniques have been developed to resolve optimization problems with complicated objectives and constraints, such as simulated annealing-based multi-objective cultural differential evolution (SAMOCDE) [20], multi-objective particle swarm optimization (MOPSO) algorithm [21], modified bacteria foraging algorithm (MBFA) [22], adaptive chaotic artificial bee colony (ACABC) algorithm [23] and evolutionary predator and prey strategy (EPPS) algorithm [24].

Recently, the Longyangxia complementary hydro-photovoltaic power plants have been selected as a case study in many studies as a representative example of the combined operation of hydropower and renewable energy power. An et al. [25] considered that hydropower can improve the power quality of photovoltaic by compensating for the intermittent and random output of PV. Ming et al. [26] presented an optimization model for complementary hydro-photovoltaic power operation that could provide effective power generation plans for a hybrid system within a reasonable time. These studies provide a reference for solving the problem of large-scale renewable energy integrated into the power grid. Nevertheless, in a large power grid, it is difficult to match the corresponding hydropower plants or other flexibly regulated power sources for all renewable energy power plants. Then, the combined operation mode of the hydro-thermal-wind hybrid power grid would be deeply affected after large-scale wind power was integrated into the power grid. Hence, it is necessary to research the optimal scheduling model of a hydro-thermal-wind hybrid system for a large power grid.

However, the traditional combined scheduling research of hydro-thermal-wind-photovoltaic hybrid power system mainly focuses on the objective function of the optimal scheduling model and the solving algorithm, while there are few studies on the combined scheduling mechanism and operation policy of hybrid power system. Compared with the traditional multipower combined operation research, this paper innovatively studies the advantages of hydro-wind compensation strategy in the combined operation of hydro-thermal-wind hybrid power system based on the principle of hydro-wind compensating operation. The main contribution of this research is to explore the role of multipower combined mechanism in guiding power grid operation.

Moreover, for addressing global warming and climate change, research on power grid combined scheduling of low carbon emissions is also important. The greenhouse effect has a decisive impact on climate change. Greenhouse gas (GHG) emissions are an important driver of the greenhouse effect. According to the Intergovernmental Panel on Climate Change (IPCC) report [27], the atmospheric concentrations of CO_2 (carbon dioxide), CH_4 (methane), and N_2O (nitrous oxide) have increased to levels unprecedented in at least the last 800,000 years. Carbon dioxide concentrations have increased by 40% since pre-industrial times, primarily from fossil fuel emissions and secondarily from net land use change emissions. In the short term, the main way to address the greenhouse effect is to reduce greenhouse gas emissions, such as carbon dioxide. Studies showed that carbon dioxide emissions in China accounted for 27.1% of emissions in the world, ranking first among all countries in 2013, and more than 80% of carbon dioxide emissions came from burning fossil fuels in China [28]. Chinese fossil fuel consumption is still dominated by coal, and 50% of coal is used for thermal power generation. Thermal power plants are a major industry that has the greatest potential to reduce emissions.

Therefore, based on the principles of hydro-wind compensation, this paper demonstrates some objectives and principles of the combined operation scheduling of a hydro-thermal-wind hybrid power system in a power grid. Then, this paper establishes the combined optimal operation model of a hydro-thermal-wind hybrid power system to obtain the optimal operation scheduling of the hybrid system. In this model, the baseload and nonbaseload output emission rates are adopted to estimate the CO_2 emissions of different power output processes and the emission reduction benefits. This work provides a theoretical basis and practical approach to the compensation operation of power plants. The remainder of this paper is organized as follows: the method of hydro-

wind compensation analysis for the power grid is introduced in Section 2; the compensating capacity of wind and hydropower in the Northwest Power Grid in China is presented in Section 3; the three scenarios of the novel operation mode and obtained simulation results are shown in Section 4. Finally, the conclusions are presented in Section 5.

2. Methods

To ensure the safe operation of the power grid after large-scale wind power is integrated into the power grid, an effective method is to compensate for the output and generation of wind power. In this paper, the combined optimal operation model of a hydro-thermal-wind hybrid power system is proposed based on the principle of hydro-wind compensating operation, the hydro-thermal-wind combined operation method and the method of carbon emission calculation for thermal power. Generally, the main contents can be formulated as follows.

2.1. The principle of hydro-wind compensating operation

Hydro-wind power compensation is superior to using the peak regulation capacity of hydropower plants to compensate for the variable output of wind power in real time. Namely, hydropower reduces its output when the wind power output increases, and water that is originally used to generate electricity can be kept in reservoirs. When the wind power output decreases, the hydropower output is instantly increased to compensate for wind power. Superposed by the compensatory output of hydropower, the intermittent and random output of wind power becomes a relatively constant value. Then, stable and reliable hydro-wind power generation is attained.

In general, hydropower stations not only conduct peak load regulation of the power grid but also compensate for the randomness and intermittency of wind power output. However, the comprehensive requirements of various water-using departments have severely restricted the regulating capacity of hydropower stations. Hence, it is necessary to make full use of hydro-wind compensation ability under the condition that hydropower curtailment is avoided. To meet the demands of water and flow for different reservoir utilization tasks and avoid hydropower curtailment, the actual power output of hydropower plants must be greater than the forced power output of hydropower ($N_{h,\ force}$). Moreover, due to the limitations of water head and installed capacity, the actual power output of hydropower plants must be less than the expected power output of hydropower ($N_{h,\ \exp ect}$). Usually, the short-term peak load regulation capacity of hydropower plants is equivalent to the difference between $N_{h,\ force}$ and $N_{h,\ \exp ect}$; the average power output of hydropower is represented as $\bar{N}_h$. For wind power plants, the power generation (E_w) and the max power output value ($N_{w,\ \max}$) of wind power have impacts on hydro-wind power compensating operation.

In Appendix A, the studies have theoretically derived the calculation formula for the capacity of hydro-wind compensating operation. However, the calculation of hydro-wind compensating operation should not only be derived from mathematical formulas but also adequately consider the operation characteristics and actual situation of hydropower plants. The economic operation of a power grid requires the full use of renewable energy and reductions in the consumption of primary energy on the basis of safe operation of the power grid. Hydropower and wind power are both clean and renewable energy. Therefore, in the combined operation process, hydropower should compensate for wind power to the maximum extent without hydropower curtailment, and the process should make full use of hydropower and wind power simultaneously. To ensure the safety of reservoirs, there are two water levels in different periods: the limited water level in the flood season and the normal water level. During the operation of hydropower plants, the water level of reservoirs must be lower than the maximum water level of the corresponding period.

The law of operation of a hydropower plant indicates that the reservoir water level is close to the water level limit or the normal water level during the flood season or the end of the storage period. Under these conditions, the average output of the hydropower plant is close to the expected output. Therefore, the storage capacity of the reservoir is very small, as is the compensation capacity of hydropower. Under the condition of no hydropower curtailment, the maximum wind power generation compensated by hydropower is represented as $E_{compensation}$.

$$E_{compensation} = (N_{h,\exp ect} - \bar{N}_h) \times 24 \tag{1}$$

When the wind power is greater than the maximum compensation power of hydropower, the wind power needs to be compensated by other power sources.

$$E_{w,uncom} = E_w - E_{compensation} = N_{w,\max} \times H - (N_{h,\exp ect} - \bar{N}_h) \times 24 \tag{2}$$

According to Eq. (2), when the average output of hydropower plants is equal to the expected output, $E_{compensation} \approx 0$. This result shows that hydropower has little compensation capacity under this condition and is totally dependent on other power sources to compensate for wind power.

2.2. The method of carbon emission calculation for thermal power

This paper adopts the “operating margin” emission factor (OM) of the electricity system, which represents kilograms of carbon dioxide equivalent per kilowatt-hour energy (kWh), to calculate the carbon dioxide emissions of the hydro-thermal-wind power system combined with combined operation [29]. The computing method of OM factor is described in Appendix B.

Then, in this paper, the nonbaseload output emission rate is adopted to estimate the carbon dioxide emissions of different processes of thermal power output and the emission reduction benefits from energy efficiency and clean energy projects. The calculation methods of nonbaseload output emission rates were further researched by Rothschild and Pechan. [30] Due to the diurnal and seasonal changes in electricity demand, the power load could be divided into baseload and nonbaseload. Baseload is defined as the minimum level of demand on an electrical grid over 24 h; the nonbaseload hourly profile is determined by subtracting the minimum load from the hourly demand load [31]. Baseload power generation and nonbaseload power generation of thermal power are represented as $E_{t,BL}$ and $E_{t,nBL}$, respectively, and $E_{t,BL}$ and $E_{t,nBL}$ can be calculated by the following formulas:

$$E_{t,BL} = T \cdot \min(N_t) \tag{3}$$

$$E_{t,nBL} = \sum [N_t - \min(N_t)] \times \Delta t \tag{4}$$

where, N_t represents the thermal power output, T represents the time of all scheduling period, and Δt represents the minimum time-scale. In this paper, the scheduling period is 1 day (24 h), and the minimum time-scale is 1 h. Then, the real physical meaning of Eq. (3) is the product of minimum power output of thermal power and all scheduling period, and the real physical meaning of Eq. (4) is the difference between all power generation and baseload power generation of thermal power.

According to the Technical Support Document for eGRID2016 [32] and the literature [29], the nonbaseload emission rates are a slice of the total system mix, with a greater weight given to plants that operate coincident with peak demand for electricity. The eGRID subregion CO_2 nonbaseload output emission rate data are recorded in the Emissions & Generation Resource Integrated Database.

Then, the CO_2 nonbaseload output emissions (Em_{nBL}) and the CO_2 baseload output emissions (Em_{BL}) can be calculated by the following formulas:

$$Em_{BL} = (E_{t,BL}) \times (EF_{\mathrm{OMsimple}}) \tag{5}$$

$$Em_{nBL} = (E_{t,nBL}) \times (EF_{\mathrm{OM,nBL}}) \tag{6}$$

where, EF_{OMsimple} represents the baseload OM factor of the power grid,

comparing with "the simple operating margin CO_2 emission factor in year y $EF_{grid,OMsimple,y}$" in the Appendix B, $EF_{OMsimple}$ confirmed the power grid and year. Then, $EF_{OM,nBL}$ represents the nonbaseload OM factor of the power grid. Then, the practical interpretation of Eqs. (5) and (6) are the product of power generation and OM factor of baseload and nonbaseload respectively.

2.3. The hydro-thermal-wind combined operation based on the principle of hydro-wind compensation

According to the principle mentioned in Section 2.1 and Appendix A, in the actual operation of the power grid, adjustable and flexible hydropower is preferentially used to regulate the peak load of the power grid. However, after the hydro-wind power compensating operation, the superposition of hydropower and wind power forms a basic constant output, and the change in hydropower reduces the capacity of peak load regulation for the power grid. Therefore, to meet the peak load regulation for the power grid, other power sources must increase the depth of peak load regulation. If the depth of the thermal power peak load regulation ($Depth$) exceeds its maximum allowable thermal power peak load regulation ($Depth_{max}$), it will lead to the thermal power regulation of the peak load by start-stop units, but this regulating operation is undoubtedly very uneconomical. In this case, to avoid the phenomenon of thermal peak load regulation by start-stop units, it is necessary to properly reduce the adjustable hydropower power, which is used to compensate wind power, and set aside part of the adjustable hydropower for peak load regulation of the power grid. Then, wind power curtailment is represented as $E_{w,curtail}$. Therefore, this paper takes the following steps to calculate and analyze the hydro-thermal-wind combined operation of a power grid based on hydro-wind power compensation. And the flowchart of hydro-thermal-wind combined operation is shown in Fig. 1.

(1) Determine the maximum compensated power output and generation of wind power by hydropower according to the hydro energy characteristics of the hydropower plant;
(2) Carry out the system load calculation and determine the depth of thermal power peak load regulation;
(3) Determine the optimal capacity of hydro-wind power compensation and analyze the depth of thermal power peak load regulation. If the depth of thermal power peak load regulation is less than its maximum value, the capacity of hydro-wind power compensation has reached its optimum value; otherwise, proceed to the next step;
(4) Reduce the power output and generation of wind power compensated by hydropower and repeat the second step calculation. Then, if the depth of thermal power peak load regulation is less than the maximum allowable thermal power peak load regulation, the capacity of hydro-wind power compensation has reached the optimal value. Otherwise, curtail a portion of wind power appropriately, and reduce the compensation of wind power output further. Then, repeat the second step and calculate again until the depth of thermal power peak load regulation is lower than its maximum capacity.

To analyze the complementary combined operation results and compare the power generation modes of the three scenarios, several factors of the consumed power profile and generated power profile are selected. The range of thermal output ($N_{t,range}$) and the depth of thermal power peak load regulation ($Depth$) represent the maximum fluctuation range of the hourly thermal power output curve for the monthly typical day and are expressed in Eqs. (7 and 8). The parameter $Depth$ is defined in the $0 \leqslant Depth \leqslant Depth_{max}$ range. For the ideal mode, $Depth$ is equal to zero, which indicates that the thermal power plants are in optimal operating conditions during the operation period. The ramping velocity of thermal power (N_{ramp}) represents the smoothness and stability of the hourly thermal power output curve and is expressed in Eq. (9). The output factor of thermal power (OF_t) represents the idle capacity of the power-on thermal power units and is expressed in Eq. (10). The output factor of thermal power can distinctly express the situation of thermal power-on capacity utilization. The parameter OF_t is defined in the $0 \leqslant OF_t \leqslant 1$ range, and if OF_t is closer to 1, the capacity utilization of thermal power units is higher.

$$N_{t,range} = N_{t,range} - N_{t,\min} \tag{7}$$

$$Depth = N_{t,range}/N_{t,\max} \tag{8}$$

$$N_{ramp} = \max |N^t_{thermal} - N^{t-1}_{thermal}|_{t = all\ the\ period} \tag{9}$$

$$OF_t = E_t/(T \times N_{t,\max}) = \frac{\sum_T N^t_{thermal}}{T \times N_{t,\max}} \tag{10}$$

where, $N_{t,\max}$ represents the maximum thermal power output, $N_{t,\min}$ represents the minimum thermal power output, E_t represents the thermal power generation, N^t_{thrmal} represents the thermal power output at t hour.

2.4. The optimal operation model based on minimizing carbon dioxide emissions

By means of the hydro-wind power compensating operation, the wind power and hydropower are superposed as relatively constant values to serve as baseloads. Under these circumstances, thermal power and the remaining hydropower are used for the remaining load of the power grid. Hence, the optimal or most profitable output process of thermal power and the remaining hydropower is another key issue of the combined operation of a hydro-thermal-wind hybrid power system. In this paper, the optimal operation model based on minimizing CO_2 emissions is proposed to solve the optimal output process of thermal power and the remaining hydropower.

The optimal output process of thermal power and the remaining hydropower can be obtained by minimizing the total CO_2 emissions of the hydro-thermal-wind hybrid power system. In this optimization, the decision variables are the hourly output of thermal power and the remaining hydropower. Then, the constraints of this issue include the fundamental operational and physical limitations of hydropower, wind power and thermal power, the generation limits of hydropower and thermal power, the consumed and generated load balance constraint, and the constraint of electricity demand.

The objective function minimizes the sum of the CO_2 emissions (Em_{total}) during the whole time period:

$$\min Em_{total} = \sum_t E_{nBL,t} + E_{BL,t} \tag{11}$$

The constraints of this issue are as follows:

(a) The fundamental operational and physical limitations of hydropower, including the physical limitations on power output constraints.

$$N_{h,force} \leqslant N^t_h \leqslant N_{h,ecpect} \tag{12}$$

where N^t_h represents the power output of hydropower at time t in the power grid.

(b) The fundamental operational and physical limitations of thermal power, including the constraint of allowable depth of peak load regulation and the constraint of the maximal allowable ramping velocity of thermal power.

$$|N^t_{thermal} - N^{t-1}_{thermal}| \leqslant N'_{ramp} \tag{13}$$

$$(N^{\max}_{thermal} - N^{\min}_{thermal})/N^{\max}_{thermal} \leqslant Depth_{\max} \tag{14}$$

where $N^t_{thermal}$ represents the power output of thermal power at time t in

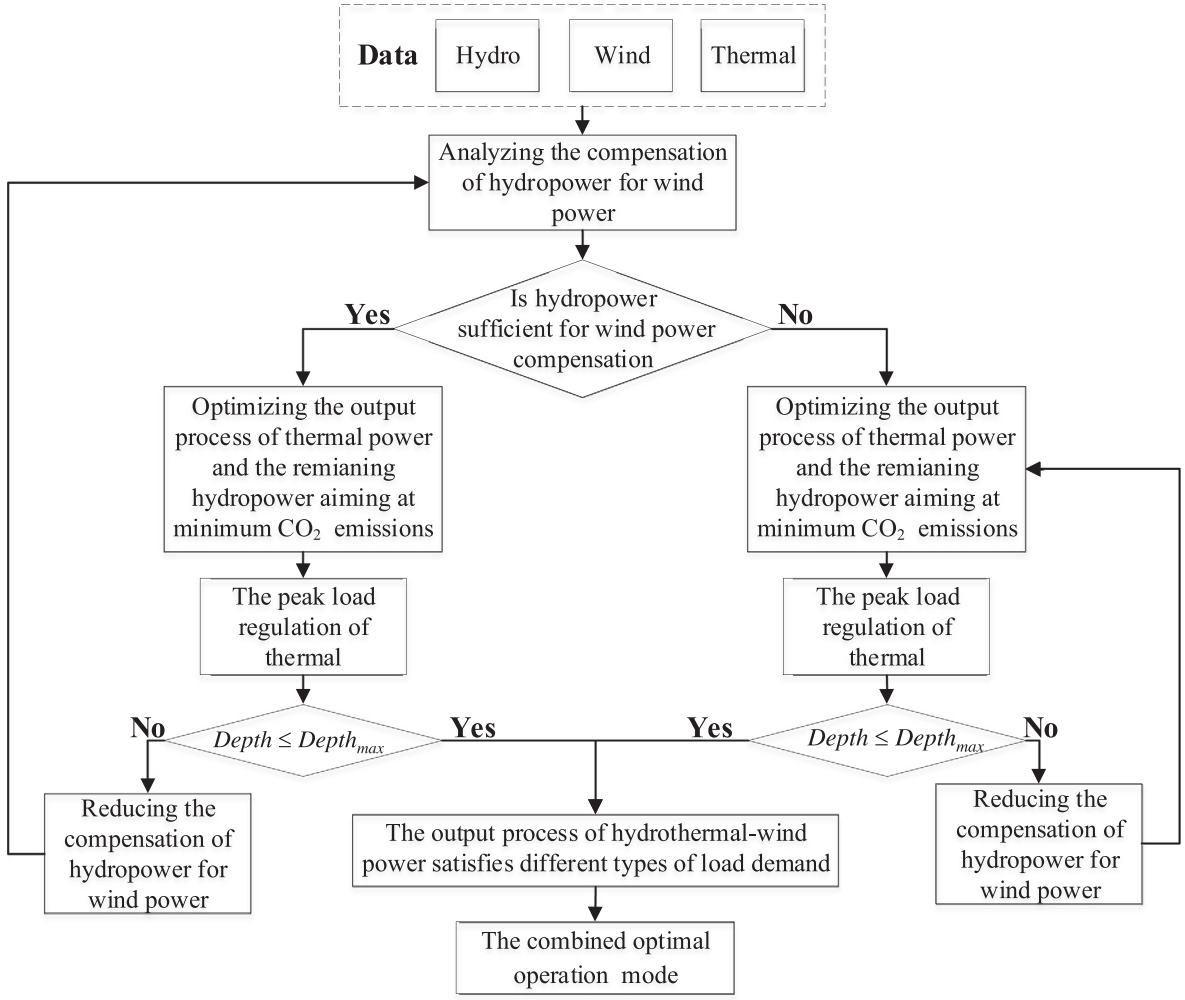

Fig. 1. Flowchart of the hydro-thermal-wind combined operation model.

the power grid and N'_{ramp} represents the maximal allowable ramping velocity of thermal power.

(c) The consumed and generated load balance constraint.

$$N_h^t + N_{thermal}^t + N_w^t = N_{total\ load}^t \tag{15}$$

where $N_{thermal}^t$ represents the power output of wind power at time t in the power grid.

3. Case study

In this section, the overviews and characteristics of Northwest Power Grid is briefly described. Then, three scenarios of hydro-thermal-wind hybrid power system combined operation are proposed to demonstrate the applicability of the hydro-wind power compensating principle in practice.

3.1. Overview of the Northwest power grid in China

The Northwest Power Grid is one of the largest power grids in China. Required data are provided by Northwest China Grid Company Limited. The installed capacity distribution of the Northwest Power Grid from 2013 to 2015 is shown in Fig. 2. The characteristics of the mean value of the generated and consumed loads of the Northwest Power Grid for the monthly typical day are shown in Fig. 3. As shown in Fig. 2, from 2013 to 2015, the installed capacity of thermal power in the Northwest Power Grid accounted for more than 50%, so thermal power is still the most important power source in the Northwest Power Grid. However, the installed capacity is increasing slowly, and the proportion has declined year by year. Because water resources are increasingly depleted in northwest China, it is not appropriate to build massive hydropower plants. Although the installed capacity grows continuously, the growth rate has been declining. In 2015, the growth rate of hydropower was only 1%. Wind energy resources and solar energy resources in the northwest region are relatively abundant. In recent years, the installed capacity of new energy has grown rapidly. By the end of 2015, the installed capacity of wind power and photovoltaic power reached 36,476 MW and 19,707 MW, respectively. The proportion of wind power in the total power sources exceeded that of hydropower in 2015. In summary, the Northwest Power Grid is dominated by thermal power, but the proportions of installed capacity of hydropower and thermal power have gradually been reduced, and the proportion of new energy installed capacity has increased. This is also an optimized reflection of the power source structure in the Northwest Power Grid.

In 2015, the proportion of wind and photovoltaic power are 17% and 10% respectively. Compared with that of wind power, the proportion of photovoltaic power installed capacity is small. Then, the randomness, intermittency and volatility of photovoltaic power are low, and the demand of hydro-photovoltaic compensating operation is relatively low too. On the other hand, the characteristics of wind and photovoltaic power are different, and the classic days of wind and

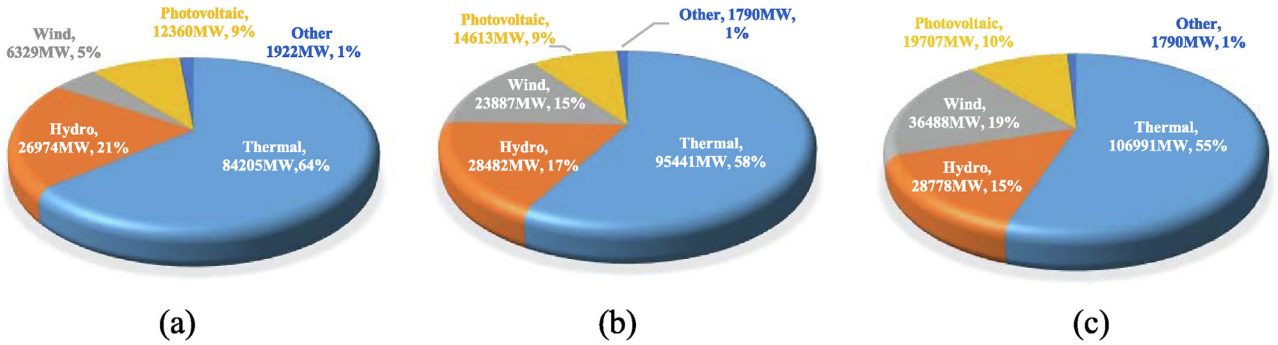

Fig. 2. Distribution diagram of installed capacity distribution in the Northwest Power Grid from 2013 to 2015.

photovoltaic power are difficult to determine. Therefore, the photovoltaic power is not selected in this paper.

3.2. The characteristics of the Northwest power grid

3.2.1. Hydropower characteristics

Hydropower plants in the Northwest Power Grid that have regulating capacity are mainly concentrated in the upstream reaches of the Yellow River. The upstream segment of the Yellow River is located from the riverhead to Inner Mongolia's Hekou town. It is the “rich ore area” of water resources and hydro energy of the Yellow River and is one of the top 12 Chinese hydropower bases. At present, the upper reaches of the Yellow River encompass more than 20 massive water conservancy hubs. In addition, the comprehensive utilization tasks of hydropower plants in the upper reaches of the Yellow River mainly include flood control, ice-flood protection, water supply and irrigation as well as water use in the middle and lower reaches [33]. Fig. 3 represents the power output curves of the Northwest Power Grid in 2015 and the proportion of each power source’s output in the power grid. The annual maximum output of hydropower is mainly concentrated in July and August, and the minimum output is mainly concentrated in December and January. To avoid hydropower curtailment, hydropower plants will increase the discharge flow in the flood season and agricultural irrigation season. The hydropower generating units have full or nearly full installed capacity operation at these times. Therefore, the hydropower output is relatively stable and is mainly used as baseload in the operation of the power grid. In the non-agricultural irrigation season of the flat and dry periods, there is less incoming water, and the hydropower plants reduce their daily power output, so hydropower has a great regulating capacity. To utilize the excellent peak-load regulation capacity of hydropower, hydropower is currently used for peak load regulation of a power grid.

3.2.2. Thermal power characteristics

As shown in Fig. 3, the power sources of the Northwest Power Grid are mainly based on thermal power, and the output of thermal power is much higher than that of other power sources. The maximum output of thermal power is mainly concentrated in December and January, and the minimum output is concentrated in August. Due to limitations of the minimum technical output of the generating units, the regulating range of thermal power output is small, and the ramping velocity is slow. Thus, the ramping velocity is the main constraint for thermal power, and the ramping of thermal power is represented by N_{ramping}. Then, in this paper, according to the thermal power characteristics of the Northwest Power Grid, the maximum allowable thermal power peak load regulation is determined as $Depth_{\max} = 0.2$. In addition, thermal power has high cost and is difficult to use for peak load regulation. Generally, it is used as the baseload in the power grid, and it takes more fuel to be used for peak load.

3.2.3. Wind power characteristics

The vast area of northwestern China, with rich wind energy and other new energy resources, is one of the most wind-rich areas in China. The wind energy resources in northwestern China are mainly concentrated in Dabancheng, the Hexi Corridor, and some mountain passes and lakes. The characteristics of wind power generation have obvious differences in different seasons, and climate factors have a great influence on wind power generation. The northwestern region has strong winds in winter and slightly weaker winds in summer. Wind power generation is greatly affected by the natural environment. Then, the wind power compensated by other power sources is suitably used as baseload in the power grid.

3.2.4. Carbon emission rate

The data on the power supply and fuel consumption in the OM calculation follow the conservative principle of the IPCC report in 2006. The OM factors of the power grid in China are shown in Table 1.

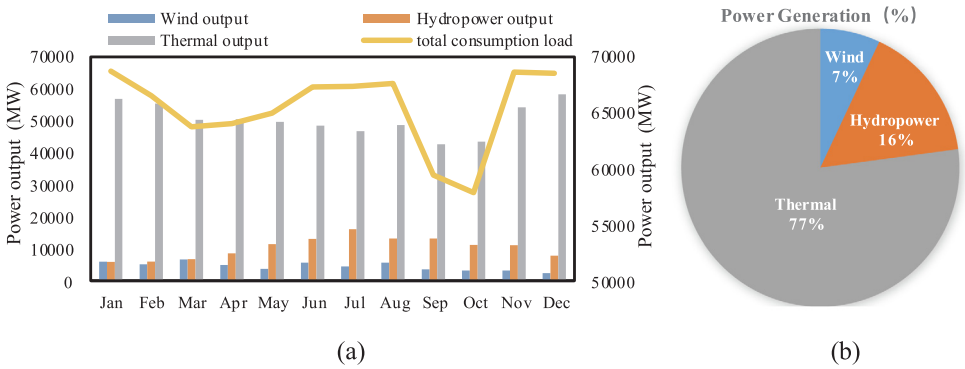

Fig. 3. Characteristics of power output and generation of the Northwest Power Grid in 2015. (a) The mean value of generated and consumed loads of the Northwest Power Grid in 2015. (b) The yearly generation of entire power sources in the Northwest Power Grid in 2015.

Table 1
The OM factors of the Northwest Power Grid in China.

Main Power Grid of China	The OM Factors of the Grid (t/MWh)			
	2012	2013	2014	Mean
the North China Power Grid	1.0583	0.9913	0.9551	1
the Northeast Power Grid	1.1225	1.1102	1.1184	1.1171
the Eastern Power Grid	0.8107	0.8222	0.7932	0.8086
the Central China Power Grid	0.9437	0.9291	0.8976	0.9229
the Northwest Power Grid	0.9546	0.9424	0.9041	0.9316
the South Power Grid	0.9063	0.8664	0.8306	0.8676

In this paper, the OM factor is used as the mean OM factor of the Northwest Power Grid from 2012 to 2014, $EF_{\mathrm{OMsimple}} = 0.9316$. Because the Northwest Power Grid of China lacks statistical data on CO_2 nonbaseload output emission rates, the CO_2 nonbaseload output emission rate can be estimated by regressing the relationship between the nonbaseload emission rate and total emission rate. In this paper, the nonbaseload OM factor of the Northwest Power Grid is determined as $EF_{\mathrm{OM},nBL} = 1.4259$.

3.3. Three scenarios of hydro-thermal-wind hybrid power system combined operation

In this paper, three scenarios of the novel operation mode are proposed to demonstrate the applicability of the hydro-wind power compensating principle in hydro-thermal-wind power combined operation. The results of hydro-thermal-wind power combined operation based on the hydro-wind power compensating principle in the Northwest Power Grid are presented. Then, the graph explanations of scenario 1, scenario 2 and scenario 3 are shown in Fig. 4.

In scenario 1, the adjustable power output and generation of hydropower fully compensate for wind power. When arranging the daily operation scheduling, the wind power is considered to participate in the generation scheduling together with other conventional power sources. According to the hydro-wind power compensating principle, the adjustable power output and generation of hydropower should be given full play to compensate for wind power generation. However, the adjusting ability of power output and generation of hydropower can't be used up at the same time. Then, when the adjustable power output of hydropower is used up, the remaining hydropower generation is used to regulate the peak load. Furthermore, if the power output and generation of wind power cannot be fully compensated by hydropower, the uncompensated power output and generation of wind power should be compensated by other power sources or curtailed when other power sources should undertake the task of peak load regulation. In this case, the adjustable power output and generation of hydropower are completely used to compensate wind power, and hydropower is no longer used to regulate the peak load of the power grid, which may lead to wasting the adjustable capacity of hydropower.

In scenario 2, assume that the wind power output process extremely deteriorates the dummy load process; then, the operation mode is the same as scenario 1. This assumption means that the wind power output is very high in times of low consumed load and it is very low in times of high consumed load. Hence, the wind power output maximizes the peak-to-valley difference of the dummy load. In such a situation, as in scenario 1, adopt the adjustable power output and generation of hydropower to compensate for the lowest wind power output. Then, the remaining hydropower and thermal power share the peak load regulation task. The output and generation of uncompensated wind power can be compensated by thermal or curtailed according to the actual situation.

In scenario 3, the adjustable power output and generation of hydropower are used to compensate for the wind power appropriately, and the remaining adjustable power output and generation are used to participate in the peak load regulating operation at the same time. In this scenario, the optimization algorithm is used to arrange the power generation mode of the power grid. The objective of determining the hydro-thermal-wind combined operation process for minimum carbon emissions is mathematically formulated using GA method. The objective is to maximize wind power generation and minimize carbon emissions. In this optimization, scheduling the peak load regulation of a hydro-thermal-wind combined system is given particular attention. The decision variables are the output of wind power, compensation of hydropower and thermal power, peak load regulation of the remaining hydropower, and remaining thermal power. The constraints of this issue include the fundamental operational and physical limitations of hydropower, wind power and thermal power, the generation limits of hydropower and thermal power, the consumed and generated load balance constraint, and the constraint of electricity demand.

4. Results and discussion

In this paper, three scenarios of the daily operation mode are built to verify the effectiveness and superiority of the combined optimal operation comparing with the actual historical operating data. The hydro-wind compensating ability, power generation, wind power curtailment, CO_2 emissions, thermal power output fluctuation and the typical operation process are demonstrated. In addition, the results of this study are also compared with the previous studies to analyze the rationality and contribution of the proposed approach.

4.1. The wind and hydropower compensation analysis for the Northwest power grid

The capacity of the hydro-wind compensating operation in the Northwest Power Grid is analyzed according to the principle (in Section 2.1). Then, the hydropower data of adjustable regulation in the Northwest Power Grid are shown in Table 2. Based on the above data of the hydropower and wind power characteristics, the monthly compensated wind power output and generation in the Northwest Power Grid are respectively calculated using the principle of hydro-wind compensating operation. The final results are exhibited in Table 3.

As shown in Tables 2 and 3, the installed capacity of wind power exceeds the installed capacity of hydropower in the Northwest Power Grid. Thus, hydropower cannot completely compensate for the power output and generation of wind power. Because of the large amount of incoming water in the flood season, the output of hydropower plants is likely to reach full capacity. Then, this effect will possibly result in hydropower curtailment when hydro-wind compensation operates. Therefore, it is recommended that other power sources be involved in wind power compensation. However, based on the principle of hydro-wind compensation, the hydro-thermal-wind combined operation of hybrid power system is beneficial to make full use of the regulation capacity of hydropower.

4.2. Power generation and wind power integration

The power generation of different power sources and the maximum integrated output of wind power under each scenario are shown in Table 4, and the power generation and wind power integration are shown in Fig. 5 and Fig. 6.

As shown in Table 4 and Figs. 5 and 6, the three scenarios of the daily operation mode could satisfy the consumed load and power generation of the Northwest Power Grid. The power output process and generation of three scenarios are consistent with the actual operating situation of the Northwest Power Grid.

The wind power generation of the three scenarios is greater than the actual historical operating data. The maximum integrated output of the wind power of the three scenarios is also greater than the actual historical operating data. These results mean that the combined operation

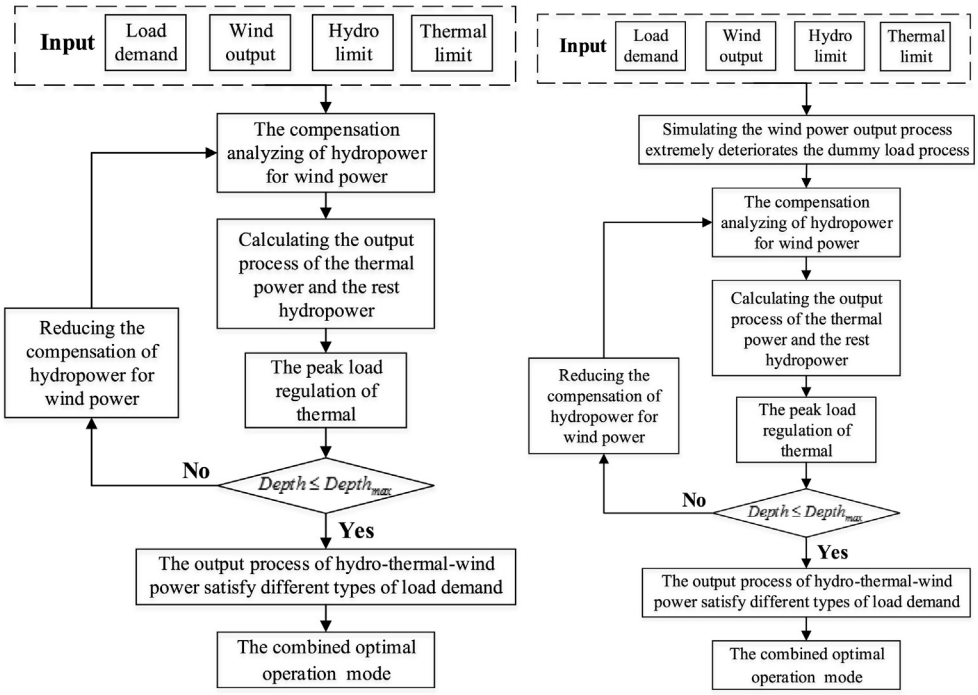

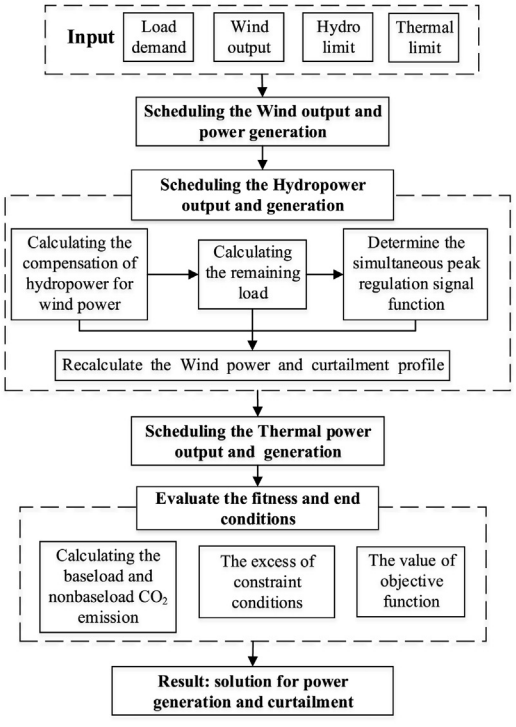

Fig. 4. The Graph explanations of scenario 1, scenario 2 and scenario 3.

Table 2
Hydro energy characteristics of the Northwest Power Grid in China in 2015.

Power Output	Jan	Feb	Mar	Apr	May	Jun	Jul	Aug	Sep	Oct	Nov	Dec
Force Power Output (MW)	3504	2753	3147	6254	8135	9855	11,362	9092	8166	7173	5280	3956
Average Power Output (MW)	5906	6018	6771	8613	11,528	13,120	16,109	13,251	13,237	11,181	11,154	7865
Expected Power output (MW)	9144	9559	11,819	13,894	14,355	17,105	19,502	16,775	16,775	14,024	13,705	11,134

Table 3
The characteristics of power output and generation of hydro-wind compensation.

	Jan	Feb	Mar	Apr	May	Jun	Jul	Aug	Sep	Oct	Nov	Dec
$N_{w,com}$(MW)	5641	6806	8672	7639	6220	7250	8140	7683	7327	6558	4189	5621
$E_{w,com}$(MWh)	57,654	78,357	86,989	56,594	81,440	78,359	113,934	99,806	110,502	90,401	52,597	78,462
$N_{w,un}$(MW)	2626	1215	1692	413	3779	1842	1826	1405	0	0	0	0
$E_{w,un}$(MWh)	47,440	17,820	55,336	38,474	82,099	30,975	35,661	13,777	0	0	0	0
$E_{w,un}/E_w$	45.14%	18.53%	38.88%	40.47%	50.20%	28.33%	23.84%	12.13%	0%	0%	0%	0%

of a hydro-thermal-wind hybrid power system based on the hydrowind power compensating principle is an effective method to increase wind power generation and integrated output. Similar results can be found in other studies. For example, An et al. [24] found that complementary hydro-photovoltaic operation could remarkably improve the power quality of photovoltaic systems and prevent the curtailment of solar energy, and it was better able to satisfy the power system than standalone photovoltaic or hydropower plants. In addition, except for a few months, the wind power generation and the maximum wind power integrated outputs of scenario 1 and scenario 2 are the same. In addition, scenario 3 is optimal. The advantage of scenario 3 is mainly concentrated in January to July. This result shows that the peak load regulation of the power grid needs to be completely regulated by thermal power when hydropower cannot fully compensate for wind power (see Section 4.1). In this case, wind power curtailment is usually executed to guarantee the peak load regulation of the power grid.

In addition, the thermal power generation of the three scenarios is lower than the actual historical operating data. This result indicates that the combined operation of a hydro-thermal-wind hybrid power system based on the hydro-wind power compensating principle can effectively reduce the randomness and volatility of the wind power output process and eliminate the adverse impact of load demand with inconsistent wind power processes. For scenario 1 and scenario 2, the thermal power generation is basically the same. Scenario 3 has the least thermal power generation, especially when hydropower cannot fully compensate for wind power. These results show that using the regulation of hydropower can effectively reduce the idle capacity of hydropower. This effect is conducive to wind power generation integrated into a power grid.

Otherwise, the hydropower generation of all three scenarios is the same as historical operating data. Then, the monthly hydropower generation presents significant seasonal characteristics. The power generation in spring and winter is significantly lower than that in summer and autumn. The highest hydropower generation appears in July, while the lowest hydropower generation appears in January. This is consistent with the annual variation of hydro energy. However, the power generation of hydropower compensating wind power and regulating peak load exhibit a large difference for each scenario. For the actual operation, the wind power is not compensated by hydropower, and the total hydropower is used to regulate the peak load of the power grid. For scenario 1 and scenario 2, only the remaining adjustable hydropower generation is used to regulate the peak load after hydro-wind power compensation. For scenario 3, the adjustable hydropower generation is used to compensate for the wind power and regulate the peak load simultaneously. Then, the hydropower generation for peak load regulation is similar in each month. This means that the optimal hydropower generation peak load regulation is always in a small range.

Table 4
The power generation of hydro-thermal-wind power system and the maximum integrated output of the wind power.

Scenario		Jan	Feb	Mar	Apr	May	Jun	Jul	Aug	Sep	Oct	Nov	Dec
Actual	E_h(10^5MWh)	1.42	1.44	1.63	2.07	2.77	3.15	3.87	3.18	3.18	2.68	2.68	1.89
	E_t(10^5MWh)	13.6	13.3	12.1	12.1	11.9	11.6	11.2	11.7	10.2	10.4	13	14
	E_w(10^5MWh)	1.43	1.23	1.6	1.19	0.91	1.37	1.08	1.37	0.854	0.774	0.774	0.56
	$E_{h,com}$(10^5MWh)	0	0	0	0	0	0	0	0	0	0	0	0
	$E_{t,com}$(MWh)	0	0	0	0	0	0	0	0	0	0	0	0
	$E_{h,peak}$(MWh)	1.42	1.44	1.63	2.07	2.77	3.15	3.87	3.18	3.18	2.68	2.68	1.89
	$N_{w,\max}$(MW)	7306	6584	8855	6505	7198	7417	7559	7221	5734	5002	3789	4161
Scenario 1	E_h(10^5MWh)	1.42	1.44	1.63	2.07	2.77	3.15	3.87	3.18	3.17	2.68	2.68	1.89
	E_t(10^5MWh)	13.2	12.8	11.4	11.7	11.5	11.1	10.8	11.1	9.87	10.1	12.7	13.8
	E_w(10^5MWh)	1.84	1.75	2.28	1.59	1.3	1.96	1.52	1.95	1.22	1.11	1.11	0.806
	$E_{h,com}$(10^5MWh)	1.42	1.44	1.63	2.07	2.77	3.15	3.87	3.18	3.06	2.63	1.79	0.784
	$E_{t,com}$(MWh)	0	22,555	55,221	11,178	81,962	32,318	6860	31,414	0	0	0	0
	$E_{h,peak}$(MWh)	0	0	0	0	0	0	0	0	11,199	5778	88,392	15,382
	$N_{w,\max}$(MW)	10,129	11,308	15,428	9472	12,230	12,713	12,686	12,870	9688	8373	6796	6627
Scenario 2	E_h(10^5MWh)	1.42	1.44	1.63	2.07	2.77	3.15	3.87	3.18	3.17	2.68	2.68	1.89
	E_t(10^5MWh)	13.2	12.8	11.4	11.7	11.5	11.1	10.8	11.1	9.87	10.1	12.7	13.8
	E_w(10^5MWh)	1.84	1.75	2.27	1.59	1.29	1.96	1.52	1.95	1.22	1.06	1.11	0.806
	$E_{h,com}$(10^5MWh)	1.42	1.4	1.63	2.07	2.77	3.14	3.82	3	3.06	2.34	1.79	1.73
	$E_{t,com}$(MWh)	489	22,555	42,533	11,178	74,614	32,318	6860	31,414	0	0	0	0
	$E_{h,peak}$(MWh)	0	4734	0	0	0	1342	4257	17,638	11,199	34,369	88,392	15,359
	$N_{w,\max}$(MW)	10,129	11,308	14,867	9472	11,902	12,713	11,187	12,870	9688	7001	6796	6627
Scenario 3	E_h(10^5MWh)	1.42	1.44	1.63	2.07	2.77	3.15	3.87	3.18	3.18	2.68	2.68	1.89
	E_t(10^5MWh)	13	12.8	11.4	11.6	11.5	11	10.8	11.1	9.87	10.1	12.7	13.8
	E_w(10^5MWh)	2.04	1.75	2.28	1.69	1.3	1.96	1.55	1.95	1.22	1.11	1.11	0.806
	$E_{h,com}$(10^5MWh)	0.72	0.657	0.868	1.17	2.05	2.33	3.04	2.5	2.56	2.04	2.2	1.01
	$E_{t,com}$(MWh)	50,620	30,530	77,663	23,565	33,787	45,879	45,879	45,879	0	0	0	0
	$E_{h,peak}$(MWh)	69,715	78,727	75,669	89,851	71,764	81,769	82,520	67,761	61,608	64,813	47,660	87,825
	$N_{w,\max}$(MW)	12,888	11,308	15,428	11,018	12,229	12,713	12,686	12,870	9687	8373	6797	6627

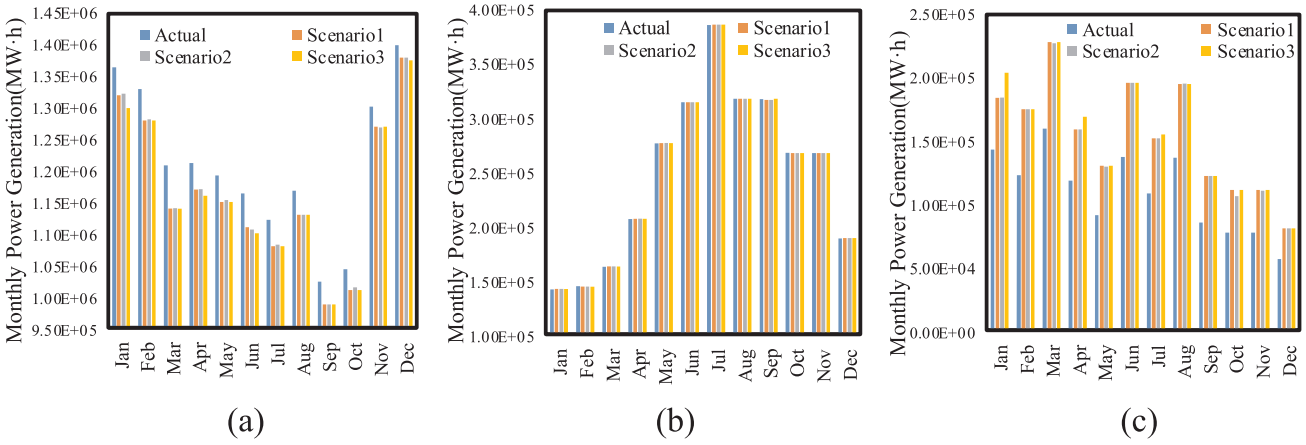

Fig. 5. The monthly power generation of hydro-thermal-wind power system. (a) Thermal power generation. (b) Hydropower generation. (c) Wind power generation.

4.3. Wind power curtailment and carbon dioxide emissions

For the actual operation and the three proposed scenarios, the results of wind power curtailment and CO_2 emissions are shown in Table 5 and Fig. 7.

As shown in Table 5 and Fig. 7, the wind power curtailment of the three scenarios is lower than the actual historical operating data. For the actual operation, the wind power curtailment occurs more in spring and less in winter. Then, the wind power curtailment of scenario 1 is similar to that of scenario 2. The difference in the wind power curtailment between scenario 1 and scenario 2 is approximately 20%. Furthermore, when there is high wind power curtailment in January and April, wind power curtailment is fully the same for scenarios 1 and 2. In addition, the monthly wind power curtailment of scenario 3 is always zero.

In addition, the CO_2 emissions of the three scenarios are lower than those in the actual historical operating data. Then, the CO_2 baseload output emissions of the three scenarios are obviously lower than those in the actual historical operating data. However, the CO_2 nonbaseload output emissions of the three scenarios are slightly greater than those in the actual operation data, especially for scenario 1 and scenario 2. The main reason is that hydropower is used to compensate for the output and power generation of wind power to the maximum extent. This use wastes the peak load regulation capacity of hydropower and increases the nonbaseload thermal power generation. For scenario 3, the flexibility of hydropower peak load regulation is fully utilized. Then, not only is wind power curtailment reduced but also CO_2 nonbaseload output emissions do not increase. Similar results can be found in other

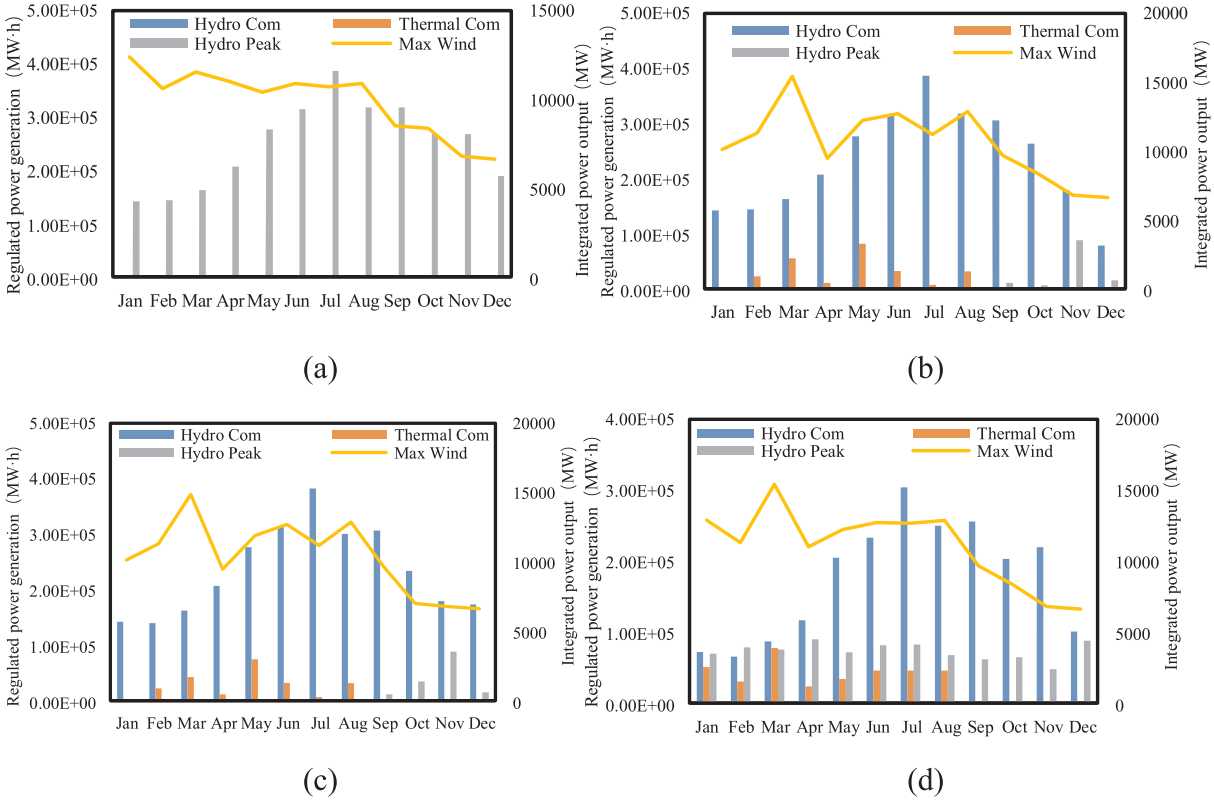

Fig. 6. The monthly power generation of hydro-thermal-wind power combined operation for three power sources. (a) The actual operation data. (b) Scenario 1. (c) Scenario 2. (d) Scenario 3.

Table 5
The wind power curtailment (MWh) and the CO_2 emissions (10^4t) in each scenario.

Scenario		Jan	Feb	Mar	Apr	May	Jun	Jul	Aug	Sep	Oct	Nov	Dec
Actual	$E_{w,curtail}$	61,264	52,565	68,385	50,807	38,991	58,735	46,463	58,591	36,600	33,167	33,160	24,175
	Em_{BL}	3623	3194	3284	3103	3179	2979	3057	3098	2666	2745	3324	3846
	Em_{nBL}	488	420	314	435	404	418	280	422	298	410	483	300
	Em	4111	3614	3598	3538	3583	3397	3337	3520	2964	3155	3807	4146
Scenario 1	$E_{w,curtail}$	19,887	0	0	10,394	0	0	0	0	0	0	0	0
	Em_{BL}	3423	3075	3085	2919	3149	2844	2839	3026	2608	2571	3413	3768
	Em_{nBL}	607	393	315	541	277	373	407	273	231	529	205	313
	Em	4031	3468	3401	3460	3426	3217	3246	3299	2838	3101	3618	4081
Scenario 2	$E_{w,curtail}$	19,887	0	780	10,394	517	0	2926	0	0	4336	0	0
	Em_{BL}	3421	3032	2927	2919	2904	2780	2817	2969	2608	2666	3386	3768
	Em_{nBL}	611	458	561	541	654	472	455	361	231	403	247	313
	Em	4032	3490	3488	3460	3558	3252	3271	3330	2838	3069	3632	4081
Scenario 3	$E_{w,curtail}$	0	0	0	0	0	0	0	0	0	0	0	0
	Em_{BL}	3482	2990	3124	2837	3158	2795	3010	2952	2582	2561	3373	3834
	Em_{nBL}	433	522	257	625	263	449	147	387	270	545	267	212
	Em	3915	3513	3381	3462	3422	3244	3156	3339	2852	3106	3639	4046

studies. For example, Xu et al. [2] proposed that a clean, reliable equilibrium scheduling model-based daily hydro-thermal-wind complementary mechanism could promote the consumption of wind power and reduce the carbon emissions of a power grid without disturbing system reliability. In addition, Li et al. [34] applied a short-term economic environmental hydro-thermal scheduling model that could provide the fuel cost and carbon emission Pareto optimal schemes of hybrid hydro-thermal power systems.

Furthermore, as seen from the distribution of monthly carbon emissions, the CO_2 emissions of the power grid are also kept at a low level during the flood season (from June to October). This result is mainly because hydro energy resources are abundant in the flood season, so hydropower can visibly reduce the demand for thermal power. At the same time, abundant hydro energy resources can effectively compensate for wind power. Then, hydropower can promote the consumption of wind power by the power grid and further reduce the baseload generation of thermal power. However, due to the flood control requirements during the flood season, the average output of hydropower is close to the expected output or hydropower installed capacity. In this case, the peak load regulation capacity of hydropower is decreased, so the nonbaseload CO_2 emissions of the power grid do not decrease during the flood season.

4.4. Thermal power output fluctuation

For the actual operation and the three proposed scenarios, the results of thermal power output fluctuations are shown in Table 6 and Fig. 8.

As shown in Table 6 and Fig. 8, the depth of the thermal power peak load regulation and the fluctuation of thermal power from high to low are represented by scenario 2 > scenario 1 > actual operation > scenario 3. Because hydropower preferentially compensates for the power output and generation of wind power, the efficiency of regulating capacity and generation of hydropower cannot be fully developed. Especially for scenario 2, as wind power is the most unfavorable output process, hydropower increases the peak load regulation demand of other power sources in the power system. Then, hydropower leads to the maximum depth of thermal power peak load regulation and fluctuation of thermal power in scenario 2. Similar results are found in previous studies with a similar scope. For example, Wang et al. [35] presented a multi-objective model for the coordinated operation of a hydro-wind-photovoltaic power system that could seek to maximize power generation and minimize output fluctuations under the constraints of multilayer architecture of the power network and balanced allocation of power curtailment.

However, the output factor of the thermal power in the three

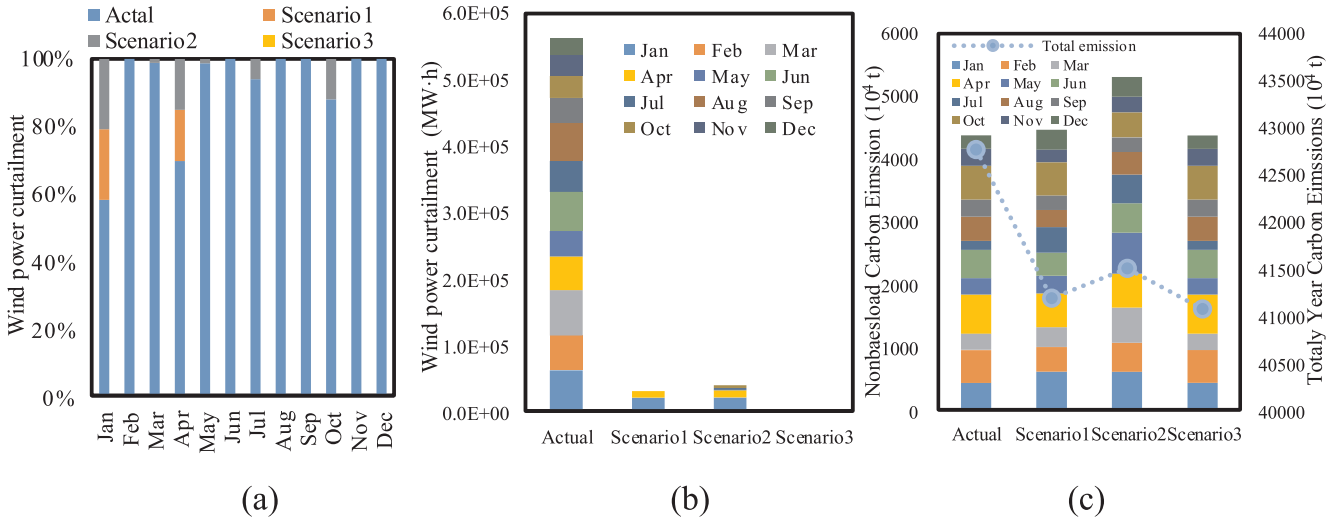

Fig. 7. The monthly wind power curtailment characteristics of hydro-thermal-wind power system. (a) The energy curtailment rate. (b) The wind power curtailment. (c) The nonbaseload carbon emissions and total carbon emissions.

Table 6
The thermal power output fluctuations in each scenario.(MW).

Scenario		Jan	Feb	Mar	Apr	May	Jun	Jul	Aug	Sep	Oct	Nov	Dec
Actual	$N_{t,range}$	8942	9216	5936	8013	7224	9097	4832	6961	5669	6932	10,669	6205
	N_{ramp}	2843	2893	2312	2797	2504	2201	1933	1294	1619	2174	3064	1938
	Depth	0.146	0.153	0.111	0.148	0.136	0.170	0.099	0.135	0.125	0.149	0.177	0.101
	OF_t	0.854	0.847	0.889	0.852	0.864	0.830	0.901	0.865	0.875	0.851	0.823	0.899
Scenario 1	$N_{t,range}$	12,256	10,851	7474	9948	6521	8687	9507	6595	4475	9028	6732	6005
	N_{ramp}	3779	3810	2658	2629	2875	3011	2138	2249	2832	3724	3607	4015
	Depth	0.199	0.176	0.166	0.186	0.143	0.159	0.195	0.131	0.103	0.196	0.117	0.099
	OF_t	0.894	0.891	0.913	0.912	0.925	0.902	0.894	0.926	0.949	0.912	0.918	0.949
Scenario 2	$N_{t,range}$	12,338	11,531	10,558	10,880	10,473	9650	10,160	7865	4763	9617	8909	9207
	N_{ramp}	3820	3631	2846	3383	4657	3865	2378	2249	2832	3732	4867	5588
	Depth	0.200	0.192	0.200	0.200	0.200	0.189	0.200	0.155	0.109	0.200	0.150	0.145
	OF_t	0.893	0.891	0.900	0.897	0.918	0.902	0.888	0.926	0.942	0.879	0.890	0.902
Scenario 3	$N_{t,range}$	7158	10,963	7893	9838	4627	9673	2655	6988	5802	9173	7329	4195
	N_{ramp}	3187	3653	4065	4000	3007	3582	1787	4652	2747	3597	2701	3389
	Depth	0.125	0.187	0.152	0.189	0.092	0.188	0.058	0.141	0.131	0.199	0.127	0.07
	OF_t	0.946	0.906	0.914	0.928	0.957	0.897	0.972	0.933	0.93	0.913	0.918	0.963

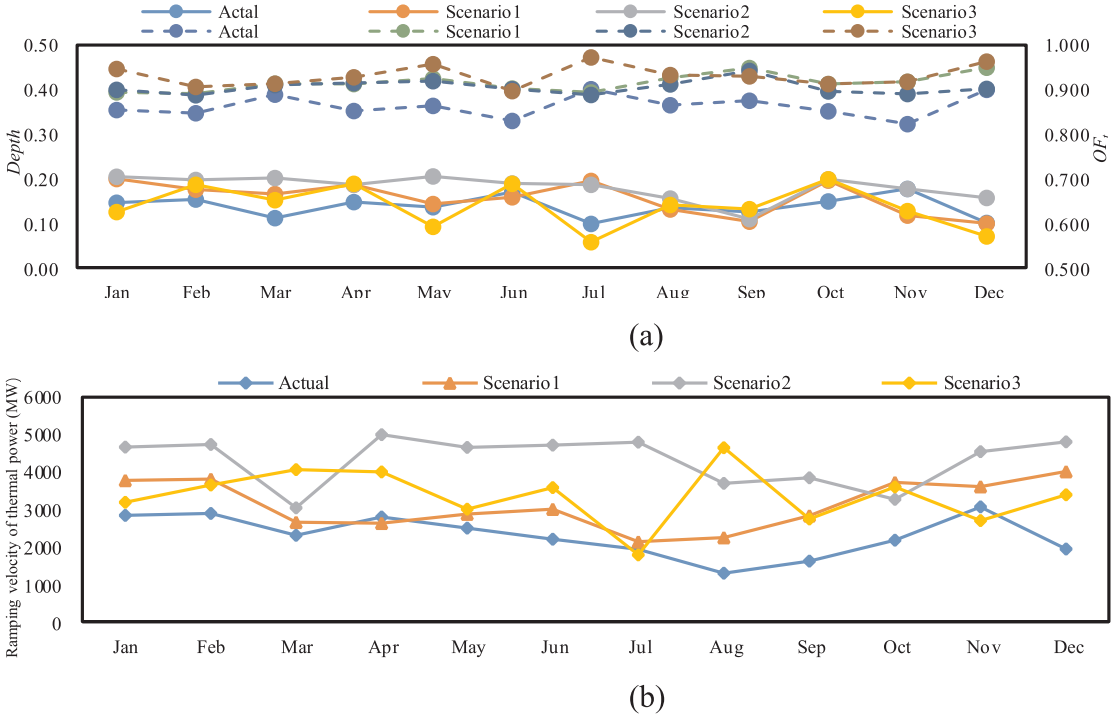

Fig. 8. The peak load regulation of thermal power. (a) The peak load regulation depth and output factor of thermal power (the solid line represents the *Depth*, and the dotted line represents the OF_t). (b) The monthly ramping velocity of thermal power.

scenarios is greater than the actual historical operating data. The output factors of the thermal power in scenario 1 and scenario 2 are similar except in winter. The output factor of the thermal power of scenario 3 is optimal. Especially in January and July, scenario 3 has significant advantages over the other scenarios. This result indicates that the thermal power of the three scenarios is closer to the full load operation. Therefore, it is conducive to the efficient operation of the thermal power unit.

4.5. Operation process of representative days

To analyze the operation process of all power sources in detail in the dry season and flood season, the representative operation process of the three scenarios in January and July are selected. The results are shown in Fig. 9.

As shown in Fig. 9, the wind power generation increases while the thermal power generation and output fluctuation decrease in the three scenarios compared to the actual operation process for both the dry season and flood season. Then, as shown in Fig. 9(a)–(d), the integrated wind power output and generation from high to low are represented by scenario 3 > scenario 1 = scenario 2 > actual operation. In contrast, the thermal power generation from high to low is represented by actual operation > scenario 1 = scenario 2 > scenario 3. Moreover, similar results can be obtained from Fig. 9(e) to (h). In addition, comparing Fig. 9(b) and (c), it is seen that the thermal power operation process is the same in scenarios 1 and 2. The operation process of wind power and hydropower is only chronologically different for scenario 1 and scenario 2. This result means that the hydro-wind compensating operation can reduce the adverse impact of randomness of wind power in the dry season. However, Fig. 9(f) and (g) show that the thermal power

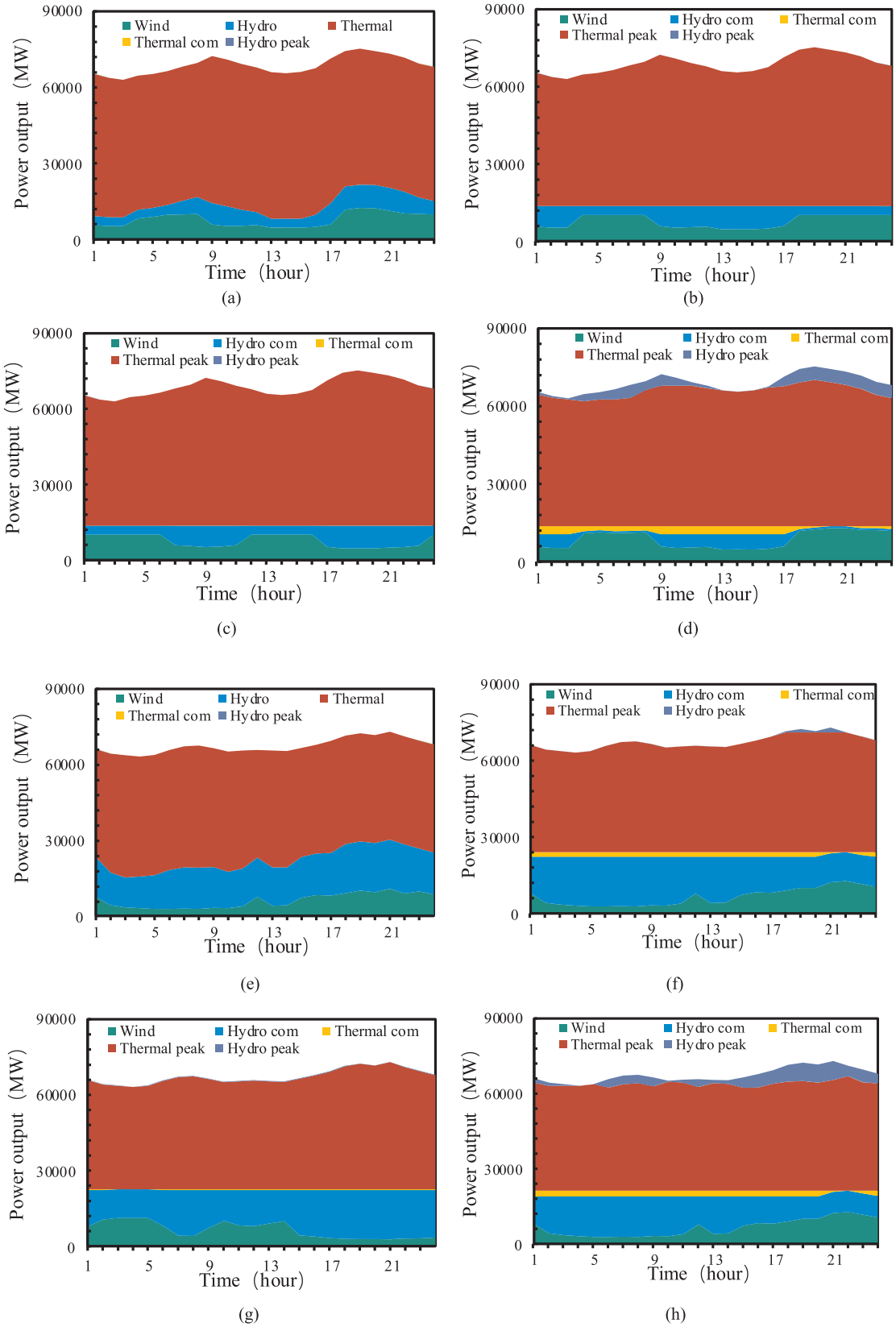

Fig. 9. The representative operation process of three scenarios in January and July. (The actual operation process in January is shown in (a); the scenario 1 operation process in January is shown in (b); the scenario 2 operation process in January is shown in (c); the scenario 3 operation process in January is shown in (d);.the actual operation process in July is shown in (e); the scenario 1 operation process in July is shown in (f); the scenario 2 operation process in July is shown in (g); and the scenario 3 operation process in July is shown in (h).)

operation process is different in the peak load period because the fluctuation of the peak load is slightly regulated by the remaining hydropower in scenario 1. Then, combining the results in Section 4.2 and Section 4.3, it can be seen that the wind power output and generation of scenario 1 are slightly greater than those of scenario 2. This result indicates that the adverse impact of the randomness of wind power cannot be fully eliminated in the flood season. Furthermore, Fig. 9(d) and (h) show that the optimal thermal power operation process appears in scenario 3 with minimum thermal power generation and the smoothest output process of thermal power.

Fig. 9 also shows the power output process of thermal and hydropower compensating wind power. Fig. 9(a) shows that the combination of hydropower and wind power sharply fluctuates. This leads to great fluctuations in thermal power. Fig. 9(b–d) show that wind power is compensated by hydropower and thermal power synchronously and that the combined output remains a constant value. Then, the compensation of thermal power is smoother than the compensation of hydropower. This result means that appropriately using thermal power for compensation of wind power has little impact on thermal power fluctuations. In the flood season, the result is similar to that of the dry season, as shown in Fig. 9(e) to (h). In addition, Fig. 9 shows that there is the best peak load regulation of hydropower in scenario 3. Both in the dry season and flood season, part of the hydropower in scenario 3 regulates the peak load demand at periods 8–10 and 18–21.

In conclusion, the combined operation scheduling of a hydro-thermal-wind hybrid power system based on the hydro-wind compensation principle proposed in this paper has shown good performance in many respects. First, it can increase wind power generation as well as decrease the power generation of thermal power and the carbon emissions of the power grid simultaneously. Second, it can take full advantage of the peak regulation capacity of hydropower plants to compensate for the intermittent and random wind power output and decrease the peak regulation requirement of thermal plants. Above all, by considering the CO_2 baseload and nonbaseload output emissions, the thermal power carbon emissions and the relationship between the carbon emissions and peak load regulation of thermal power can be quantitatively analyzed.

Compared with the traditional multipower combined operation research, the researches of other scholars are limited to the traditional power generation optimization operation, ignoring the combined scheduling operation mechanism and policy of hybrid power system. For example, Wang et al. [1] proposed a combined coordinated operation model of interconnected power systems with hydro-thermal-wind-photovoltaic (HTWP) plants to mitigate the curtailment problem of new energy by maximizing the new energy power generation and minimizing the thermal output fluctuation. However, in this work, the internal structure of power grid is less considered, and the hydro-wind compensating operation is considered as the ideal condition. The constraints of power grid and hydro-wind compensating operation should be more considered in future research.

5. Conclusions

Wind and solar energy are considered major renewable resources to address the constraints of resources and the environment for energy development. However, these new energy sources have the disadvantages of randomness, intermittency and uncontrollability. These disadvantages make large-scale wind power generation present large challenges for integration into a power grid. In this paper, based on the principles of hydro-wind compensating operation, the optimizing operation model of a hydro-thermal-wind hybrid power system is proposed to promote the integration of large-scale wind power into the power grid. In this model, the baseload and nonbaseload output emission rates are adopted to estimate the CO_2 emissions of different power output processes and the emission reduction benefits. Then, the Northwest Power Grid in China is selected as a case study, and it is used to verify the effectiveness of the proposed model and methods. The major conclusions can be drawn as follows.

(1) The proposed model can reduce the power generation and output fluctuations of thermal power and the CO_2 emissions of the power grid by the combined operation of a hydro-thermal-wind hybrid power system based on the hydro-wind power compensating principle. In particular, the CO_2 emissions could be reduced by approximately $1696*10^4$ t every year in the Northwest Power Grid.
(2) The proposed model can improve the wind power generation and alleviate the wind power curtailment by making full use of the peak load regulation capacity and the compensating characteristics of hydropower.

The results provide a reference for realizing the maximization of economic and ecological benefits in a power grid. Nevertheless, to determine the maximum integrated capacity of wind power in the Northwest Power Grid, the actual transmitted power process between the subregions and the operation process of each hydropower plant are considered as the ideal conditions in this paper. In reality, these simplifications are different from actual operating conditions. Hence, it is necessary to make the simulation process consistent with the actual operation process as much as possible and improve the rationality of the power generation plan for the power grid.

Acknowledgements

This research was supported by the National Key Research and Development Program of China [grant number 2017YFC0404404] and the Natural Science Foundation of China [grant number 91647112, 51679187, and 51679189]. The authors gratefully thank the Northwest China Grid Company Limited for providing the data. Sincere gratitude is extended to the editor and the anonymous reviewers for their professional comments and corrections.

Declaration of interest

No conflict of interest exists in the submission of this manuscript, and manuscript is approved by all the authors for publication. I now declare on behalf of my co-authors that the work described is original research that has not been published previously, and is not under consideration for publication elsewhere, in whole nor in part. It would be my honor if I am a reviewer for other articles for Energy Conversion and Management.

Appendix A:. The derivation of hydro-wind compensating calculation

The derivation of hydro-wind compensating calculation are given as follows.

According to the wind power output process on one day, the wind power output process can be roughly generalized into 3 situations, as shown in Fig. A1.

For the above three cases in Fig. A1, as long as the power generation and the max power output of wind power are known constants, the principle of hydro-wind compensating operation is identical. When the processes of wind power output are similar to the rectangle, pyramidal or actual situation in Fig. A1(a–c), respectively, the calculation method of hydro-wind compensating capacity is identical. Only the calculation formula of wind power generation needs to be corrected. Hence, to ensure derivation of a simple and clear formula, the process of wind power output can be assumed as the condition of Fig. A1(a).

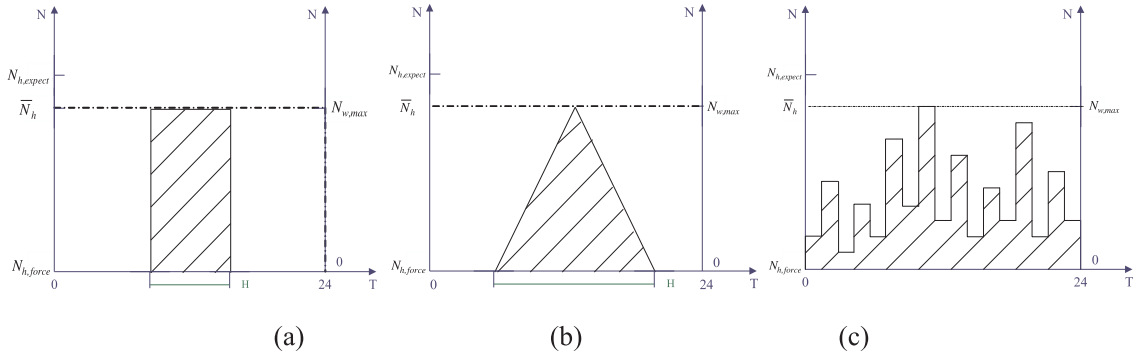

Fig. A1. The power output process of a wind power plant.

The adjustable output range is [0, $N_{h,controll}$], of which hydropower can compensate for wind power.

$$N_{h,controll} = N_{h,\exp ect} - N_{h,force} \tag{A1}$$

1. When $N_{h,controll} \geqslant N_{w,\max}$, the situation of hydropower compensating wind power is as follows:

$$E_w = N_{w,\max} \times H \tag{A2}$$

where E_w represents wind power, and H represents the time of wind power generation.

The combined power generation of hydropower and wind power is represented as E_{h-w}.

$$E_{h-w} = 24 \times N_{w,\max} \tag{A3}$$

Then, the maximum compensating power generation of hydropower for wind power is represented as E_w^*. The formula to calculate E_w^* is as follows:

$$E_w^* = E_{h-w} - E_w = 24 \times N_{w,\max} - N_{w,\max} \times H = N_{w,\max} \times (24 - H) \tag{A4}$$

The actual power generation of hydropower is represented as E_h. The maximum adjustable power generation of hydropower is represented as $E_{h,controll}$. Then, these two variates can be calculated as follows:

$$E_h = \bar{N}_h \times 24 \tag{A5}$$

$$E_{h,controll} = (\bar{N}_h - N_{h,force}) \times 24 \tag{A6}$$

(1) When $E_{h,controll} = E_w^*$, hydropower can compensate for wind power exactly, but there is no excess regulation capacity to participate in the peak load regulating operation, as shown in Fig. A2(a).
(2) When $E_{h,controll} > E_w^*$, the schematic diagram is shown in Fig. A2(b). Hydropower can completely compensate for wind power, and there is excess regulation capacity of hydropower to participate in the peak load regulating operation. $E_{h,peak}$ represents the excess hydropower generation that can participate in the peak load regulating operation.

$$E_{h,peak} = E_{h,controll} - E_w^* = (\bar{N}_h - N_{h,force}) \times 24 - N_{w,\max} \times (24 - H) \tag{A7}$$

(3) When $E_{h,controll} < E_w^*$, the schematic diagram is shown in Fig. A2(c). Hydropower cannot fully compensate for wind power, and the other power sources are required to participate in wind power compensation. The uncompensated wind power generation is represented as $E_{w,uncom}$.

$$E_{w,uncom} = E_w - \frac{E_{h,controll}}{24 - H} \times H = \left(N_{w,\max} - \frac{(\bar{N}_h - N_{h,force}) \times 24}{24 - H} \right) \times H \tag{A8}$$

Then, the remaining wind power $N_{w,uncom}$ should be compensated by other power sources, such as thermal power. The output and generation of thermal power compensating for the remaining wind power are represented by $N_{t,com}$ and $E_{t,com}$, respectively.

$$N_{t,com} = N_{t,\max} - \frac{E_{h,controll}}{24 - H} = N_{t,\max} - \frac{\bar{E}_h - E_{h,force}}{24 - H} \tag{A9}$$

$$E_{t,com} = \frac{E_{w,uncom} \times (24 - H)}{H} \tag{A10}$$

2. When $N_{h,controll} < N_{w,\max}$, the specific situation of hydro-wind compensation is shown in Fig. A2(d). Hydropower cannot fully compensate for the wind power output, and wind power needs to be compensated by other power sources. The actual power output of hydropower compensating wind power is represented as $N_{h,\ com}$.

$$N_{h,com} = \frac{N_{h,controll} \times 24}{24 - H} = \frac{(\bar{N}_h - N_{h,force}) \times 24}{24 - H} \tag{A11}$$

If $N_{h,com} < N_{h,controll}$, $E_{w,uncom}$ represents the wind power generation that cannot be compensated by hydropower. $E_{w,uncom}$ can be calculated by the following formula:

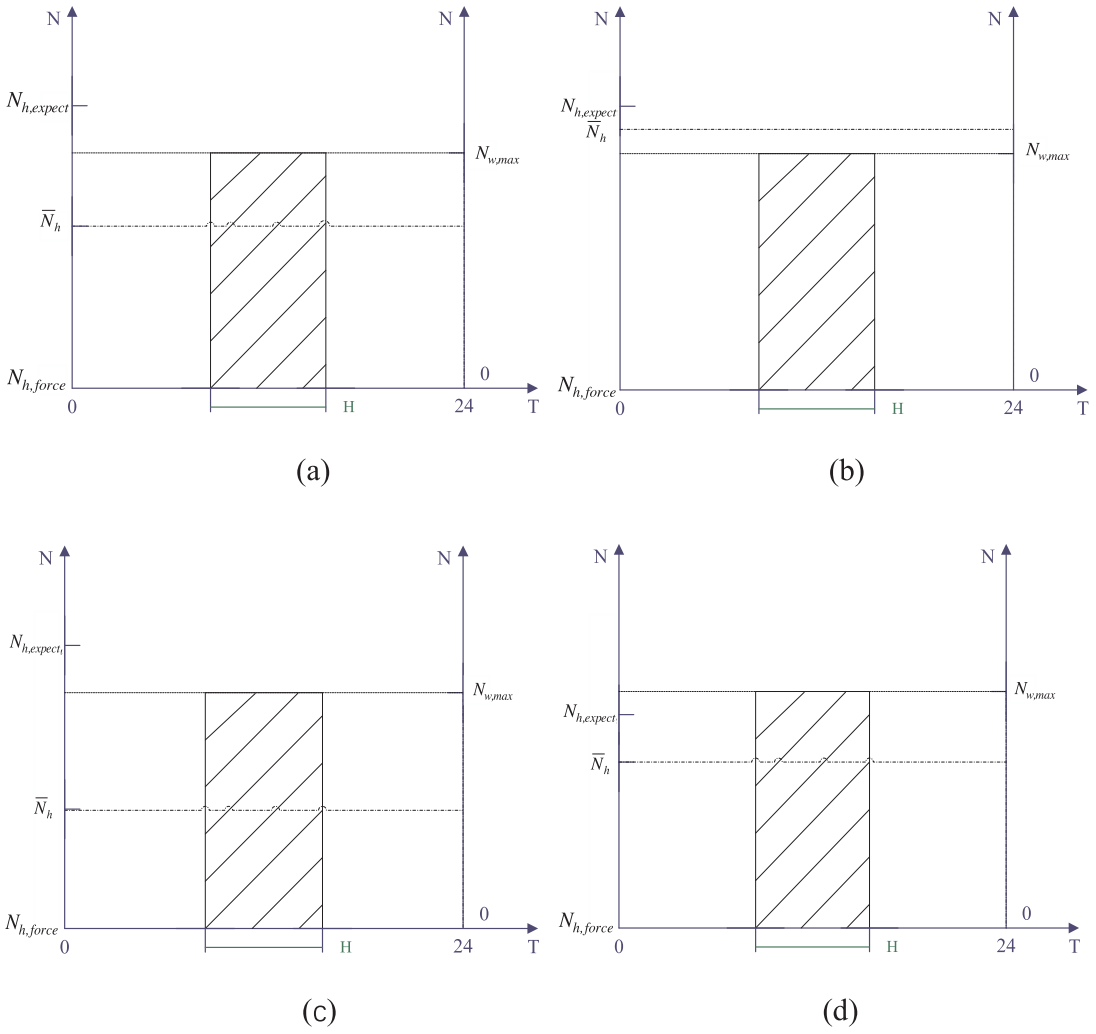

Fig. A2. Schematic of the calculation of hydro-wind compensation.

$$N_{h,com} = E_w - \frac{N_{h,controll} \times 24}{24 - H} = \left(N_{w,\max} - \frac{(\bar{N_h} - N_{h,force}) \times 24}{24 - H} \right) \times H \tag{A12}$$

If $N_{h,com} \geqslant N_{h,controll}$, then $N_{h,com} = N_{h,controll}$. The uncompensated wind power generation ($E_{w,uncom}$) can be calculated by the following formula:

$$E_{h,com} = N_{h,controll} \times (24 - H) = (N_{h,\exp ect} - N_{h,force}) \times (24 - H) \tag{A13}$$

$$E_{w,uncom} = E_w - \frac{E_{h,com}}{24 - H} \times H = (N_{w,\max} - N_{h,\exp ect} + N_{h,force}) \times H \tag{A14}$$

The above studies have theoretically derived the calculation formula for the capacity of hydro-wind compensating operation. However, the calculation of hydro-wind compensating operation should not only be derived from mathematical formulas but also adequately consider the operation characteristics and actual situation of hydropower plants. The economic operation of a power grid requires the full use of renewable energy and reductions in the consumption of primary energy on the basis of safe operation of the power grid. Hydropower and wind power are both clean and renewable energy. Therefore, in the combined operation process, hydropower should compensate for wind power to the maximum extent without hydropower curtailment, and the process should make full use of hydropower and wind power simultaneously. To ensure the safety of reservoirs, there are two water levels in different periods: the limited water level in the flood season and the normal water level. During the operation of hydropower plants, the water level of reservoirs must be lower than the maximum water level of the corresponding period.

The law of operation of a hydropower plant indicates that the reservoir water level is close to the water level limit or the normal water level during the flood season or the end of the storage period. Under these conditions, the average output of the hydropower plant is close to the expected output. Therefore, the storage capacity of the reservoir is very small, as is the compensation capacity of hydropower. Under the condition of no hydropower curtailment, the maximum wind power generation compensated by hydropower is represented as $E_{compensation}$.

$$E_{compensation} = (N_{h,\exp ect} - \bar{N_h}) \times 24 \tag{A15}$$

When the wind power is greater than the maximum compensation power of hydropower, the wind power needs to be compensated by other power sources.

$$E_{w,uncom} = E_w - E_{compensation} = N_{w,\max} \times H - (N_{h,\exp ect} - \bar{N_h}) \times 24 \tag{A16}$$

According to Eq. (A16), when the average output of hydropower plants is equal to the expected output, $E_{compensation} \approx 0$. This result shows that hydropower has little compensation capacity under this condition and is totally dependent on other power sources to compensate for wind power.

Appendix B:. The computing method of OM factor

To determine the OM factor, this paper adopts the method in the Methodological Tool, which was issued by the CDM Executive Board under the United Nations Framework Convention on Climate Change (UNFCCC), to calculate the emission factor for an electricity system. The OM emission factor is calculated based on the net electricity supplied to the grid by all thermal power plants serving the system, as well as the fuel type(s) and total fuel consumption of the power system, as follows:

$$EF_{grid,OMsimpley} = \frac{\sum_i (FC_{i,y} \times NCV_{i,y} \times EF_{CO_2 i,y})}{EG_y} \quad \text{(B1)}$$

where $EF_{\text{grid,OMsimple},y}$ represents simple operating margin CO_2 emission factor in year y (tCO_2/MWh); $FC_{i,y}$ represents amount of fossil fuel type i consumed in the project electricity system in year y (mass or volume unit); $NCV_{i,y}$ represents net calorific value (energy content) of fossil fuel type i in year y (GJ/mass or volume unit); $EF_{CO_2,i,y}$ represents CO_2 emission factor of fossil fuel type i in year y (tCO_2/GJ); EG_y represents net electricity generated and delivered to the grid by all power sources serving the system, not including low-cost/must-run power plants/units, in year y (MWh); i represents all fossil fuel types combusted in power sources in the project electricity system in year y; and y represents the relevant year as per the data vintage.

Then, the carbon dioxide emissions of thermal power in time slot y can be denoted as:

$$EM_y = EF_{grid,OMsimpley} \times G_y \quad \text{(B2)}$$

where Em_y represents the carbon dioxide emissions of thermal power, and G_y represents the power generation of thermal power.

References

[1] Wang X, Chang J, Meng X, et al. Short-term hydro-thermal-wind-photovoltaic complementary operation of interconnected power systems. Appl Energy 2018;229:945–62. https://doi.org/10.1016/j.apenergy.2018.08.034.

[2] Xu J, et al. Carbon emission reduction and reliable power supply equilibrium based daily scheduling towards hydro-thermal-wind generation system: a perspective from China. Energy Convers Manage 2018;164:1–14. https://doi.org/10.1016/j.enconman.2018.01.064.

[3] Sheng Z, Yu W, Zhou Y, et al. Roles of wind and solar energy in China's power sector: Implications of intermittency constraints. Appl Energy 2018;213:22–30. https://doi.org/10.1016/j.apenergy.2018.01.025.

[4] Amrollahi MH, Bathaee SMT. Techno-economic optimization of hybrid photovoltaic/wind generation together with energy storage system in a stand-alone micro-grid subjected to demand response. Appl Energy 2017;202. https://doi.org/10.1016/j.apenergy.2017.05.116.

[5] Fang X, Misra S, Xue G, et al. Smart grid — the new and improved power grid: a survey. IEEE Commun Surv Tutorials 2012;14(4):944–80. https://doi.org/10.1109/SURV.2011.101911.00087.

[6] Panda A, Tripathy M, Barisal AK, et al. A modified bacteria foraging based optimal power flow framework for Hydro-Thermal-Wind generation system in the presence of STATCOM. Energy 2017;124:720–40. https://doi.org/10.1016/j.energy.2017.02.090.

[7] Hui Q, Zhou J, Lu Y, et al. Multi-objective differential evolution with adaptive Cauchy mutation for short-term multi-objective optimal hydro-thermal scheduling. Energy Convers Manage 2010;51(4):788–94. https://doi.org/10.1016/j.enconman.2009.10.036.

[8] Zhang H, Chang J, Gao C, et al. Cascade hydropower plants operation considering comprehensive ecological water demands. Energy Convers Manage 2019;180:119–33. https://doi.org/10.1016/j.enconman.2018.10.072.

[9] Zhang H, Zhou J, Fang N, et al. Daily hydrothermal scheduling with economic emission using simulated annealing technique based multi-objective cultural differential evolution approach. Energy 2013;50(1):24–37. https://doi.org/10.1016/j.energy.2012.12.001.

[10] Jianxia C, Xiaoyu W, Yunyun L, et al. Hydropower plant operation rules optimization response to climate change. Energy 2018;160:886–97. https://doi.org/10.1016/j.energy.2018.07.066.

[11] Dubey HM, Pandit M, Panigrahi BK. Hydro-thermal-wind scheduling employing novel ant lion optimization technique with composite ranking index. Renew Energy 2016;99:18–34. https://doi.org/10.1016/j.renene.2016.06.039.

[12] Panda A, Tripathy M. Optimal power flow solution of wind integrated power system using modified bacteria foraging algorithm. Int J Electr Power Energy Syst 2014;54(1):306–14. https://doi.org/10.1016/j.ijepes.2013.07.018.

[13] Xuejiao M, Jianxia C, Xuebin W, Yimin W. Multi-objective hydropower station operation using an improved cuckoo search algorithm. Energy 2019;168:425–39. https://doi.org/10.1016/j.energy.2018.11.096.

[14] Yuan X, Yuan Y, Zhang Y. A hybrid chaotic genetic algorithm for short-term hydro system scheduling. Math Comput Simul 2002;59(4):319–27. https://doi.org/10.1016/S0378-4754(01)00363-9.

[15] Sinha N, Chakrabarti R, Chattopadhyay PK. Fast evolutionary programming techniques for short-term hydrothermal scheduling. Electr Power Syst Res 2003;66(2):97–103. https://doi.org/10.1016/s0378-7796(03)00016-6.

[16] Yu B, Yuan X, Wang J. Short-term hydro-thermal scheduling using particle swarm optimization method. Energy Convers Manage 2007;48(7):1902–8. https://doi.org/10.1016/j.enconman.2007.01.034.

[17] Yuan X, Zhang Y, Wang L, et al. An enhanced differential evolution algorithm for daily optimal hydro generation scheduling. Comput Math Appl 2008;55(11):2458–68. https://doi.org/10.1016/j.camwa.2007.08.040.

[18] Guo W, Peng Z. Hydropower system operation stability considering the coupling effect of water potential energy in surge tank and power grid. Renew Energy 2019;134:846–61. https://doi.org/10.1016/j.renene.2018.11.064.

[19] Yang J, Zhou J, Li L, et al. A novel strategy of pareto-optimal solution searching in multi-objective particle swarm optimization (MOPSO). Comput Math Appl 2009;57(11–12):1995–2000. https://doi.org/10.1016/j.camwa.2008.10.009.

[20] Zhang H, Yue D, Xie X, et al. Multi-elite guide hybrid differential evolution with simulated annealing technique for dynamic economic emission dispatch. Appl Soft Comput 2015;34(C):312–23. https://doi.org/10.1016/j.asoc.2015.05.012.

[21] Wang HG, Liang MA. Multi-objective particle swarm optimization. Comput Eng Appl 2008;45(4):82–5http://cea.ceaj.org/EN/10.3778/j.issn.1002-8331.2008.34.018.

[22] Panda A, Tripathy M. Security constrained optimal power flow solution of wind-thermal generation system using modified bacteria foraging algorithm. Energy 2015;93(8):816–27. https://doi.org/10.1016/j.energy.2015.09.083.

[23] Liao X, Zhou J, Ouyang S, et al. An adaptive chaotic artificial bee colony algorithm for short-term hydrothermal generation scheduling. Int J Electr Power Energy Syst 2013;53(1):34–42. https://doi.org/10.1016/j.ijepes.2013.04.004.

[24] Huber M, Weissbart C. On the optimal mix of wind and solar generation in the future Chinese power system. Energy 2015;90:235–43. https://doi.org/10.1016/j.energy.2015.05.146.

[25] An Y, Fang W, Ming B, et al. Theories and methodology of complementary hydro/photovoltaic operation: applications to short-term scheduling. J Renew Sust Energy 2015;7(6):2926–39. https://doi.org/10.1063/1.4939056.

[26] Ming B, Liu P, Cheng L, et al. Optimal daily generation scheduling of large hydro–photovoltaic hybrid power plants. Energy Convers Manage 2018;171:528–40. https://doi.org/10.1016/j.enconman.2018.06.001.

[27] Solomon S. IPCC (2007): Climate Change The Physical Science Basis. AGU Fall Meeting. AGU Fall Meeting Abstracts; 2007:123–124. https://www.researchgate.net/publication/260734292_IPCC_2007_Climate_Change_The_Physical_Science_Basis.

[28] Stocker T. IPCC, Technical Summary. In: Climate Change 2013: The Physical Science Basis. Contribution of Working Group I to the Fifth Assessment Report of the Intergovernmental Panel on Climate Change. Computat Geomet 2013;18(2):95–123.

[29] Biewald B. Using Electric System Operating Margins and Build Margins in Quantification of Carbon Emission Reductions Attributable to Grid Connected CDM Projects; 2013. https://www.researchgate.net/publication/242185101_Using_Electric_System_Operating_Margins_and_Build_Margins_in_Quantification_of_Carbon_Emission_Reductions_Attributable_to_Grid_Connected_CDM_Projects.

[30] Rothschild SS, Pechan E. Total, non-baseload, eGRID subregion, state? guidance on the use of eGRID output emission rate. U.S Environmental Protection Agency OAP, Comprehensive Inventories -Leveraging Technology and Resources 2009https://www3.epa.gov/ttn/chief/conference/ei18/session5/rothschild.pdf.

[31] Brito MC, Freitas S, Guimarães S, et al. The importance of facades for the solar PV potential of a Mediterranean city using LiDAR data. Renew Energy 2017;111:85–94. https://doi.org/10.1016/j.renene.2017.03.085.

[32] Abt Associates. Emissions & Generation Resource integrated Database (eGRID) Technical Support Document for eGRID2016 [R]. U.S. Environmental Protection

Agency. February; 2018, https://www.epa.gov/energy/emissions-generation-resource-integrated-database-egrid.
[33] Chang J, Guo A, Wang Y, et al. Reservoir operations to mitigate drought effects with a hedging policytriggered by the drought prevention limiting water level. Water Resour Res 2019. https://doi.org/10.1029/2017WR022090.
[34] Li C, Zhou J, Peng L, et al. Short-term economic environmental hydrothermal scheduling using improved multi-objective gravitational search algorithm. Energy Convers Manage 2015;89:127–36. https://doi.org/10.1016/j.enconman.2014.09.063.
[35] Wang X, Mei Y, Kong Y, et al. Improved multi-objective model and analysis of the coordinated operation of a hydro-wind-photovoltaic system. Energy 2017;134. https://doi.org/10.1016/j.energy.2017.06.047.